YALE JOURNAL OF BIOLOGY AND MEDICINE 96 (2023), pp.527-547.

REVIEW

YALE JOURNAL OF BIOLOGY AND MEDICINE
YJBM
CELEBRATING 95 YEARS 1928–2023

Advances in Regulating Cellular Behavior Using Micropatterns

Yizhou Li[a,b], Wenli Jiang[a], Xintong Zhou[a], Yicen Long[a], Yujia Sun[a], Ye Zeng[a,*], and Xinghong Yao[c,*]

[a]*Institute of Biomedical Engineering, West China School of Basic Medical Sciences and Forensic Medicine, Sichuan University, Chengdu, P.R. China;* [b]*State Key Laboratory of Oral Diseases & National Center for Stomatology & National Clinical Research Center for Oral Diseases, West China Hospital of Stomatology, Sichuan University, Chengdu, P.R. China;* [c]*Radiation Oncology Key Laboratory of Sichuan Province, Department of Radiotherapy, Sichuan Clinical Research Center for Cancer, Sichuan Cancer Hospital and Institute, Sichuan Cancer Center, Affiliated Cancer Hospital of University of Electronic Science and Technology of China, Chengdu, P.R. China*

Micropatterns, characterized as distinct physical microstructures or chemical adhesion matrices on substance surfaces, have emerged as a powerful tool for manipulating cellular activity. By creating specific extracellular matrix microenvironments, micropatterns can influence various cell behaviors, including orientation, proliferation, migration, and differentiation. This review provides a comprehensive overview of the latest advancements in the use of micropatterns for cell behavior regulation. It discusses the influence of micropattern morphology and coating on cell behavior and the underlying mechanisms. It also highlights future research directions in this field, aiming to inspire new investigations in materials medicine, regenerative medicine, and tissue engineering. The review underscores the potential of micropatterns as a novel approach for controlling cell behavior, which could pave the way for breakthroughs in various biomedical applications.

INTRODUCTION

Cells maintain extensive connections to their extracellular matrix (ECM) microenvironment, and their behaviors can be modulated by a variety of physical, chemical, and mechanical stimuli present in their surroundings [1-12]. The heightened sensitivity of cells to the mechanical and biochemical properties of their external microenvironment highlights the inadequacy of conventional cell culture platforms, underscoring the need for culture models with enhanced physiological relevance [13,14].

Micropatterning, a microfabrication technique that

*To whom all correspondence should be addressed: Ye Zeng, Sichuan University, Chengdu, Sichuan, P.R. China, Email: ye@scu.edu.cn. Xinghong Yao, Sichuan Cancer Hospital and Institute, Chengdu, Sichuan, P.R. China, Email: yaoxingho@126.com.

Abbreviations: ECM, extracellular matrix; PDMS, polydimethylsiloxane; LIMAP, light-induced molecular adsorption of proteins; PVA, polyvinyl alcohol; PEG, polyethylene glycol; RGD, arginine-glycine-aspartate; PLCL, poly(L-lactide-co-ε-caprolactone); MDCK, Madin-Darby canine kidney; BMSC, bone marrow mesenchymal stem cells; PLGA, poly(lactic-co-glycolic acid); ECs, endothelial cells; FSS, fluid shear stress; hPSCs, human pluripotent stem cells; MSCs, human mesenchymal stem cells; HUVECs, human umbilical vein endothelial cells; p-FAK, phosphorylated adherents spot kinase; YAP, yes-associated protein; VSMCs, vascular smooth muscle cells; RGE, arginine-glycine-glutamate; ROCK, Rho-associated kinase; NICD, Notch intracellular domain; TAZ, transcriptional coactivator with PDZ-binding motif; TEAD, transcriptional enhanced associate domain; LINC, Linker of Nucleoskeleton and Cytoskeleton; hWJ-MSCs, human Wharton's jelly MSCs.

Keywords: microenvironment, micropattern, extracellular matrix, cell behavior

Author Contributions: YZ and XHY contributed to the conception of the work. YZ and YL drafted the manuscript. All authors approved the final manuscript.

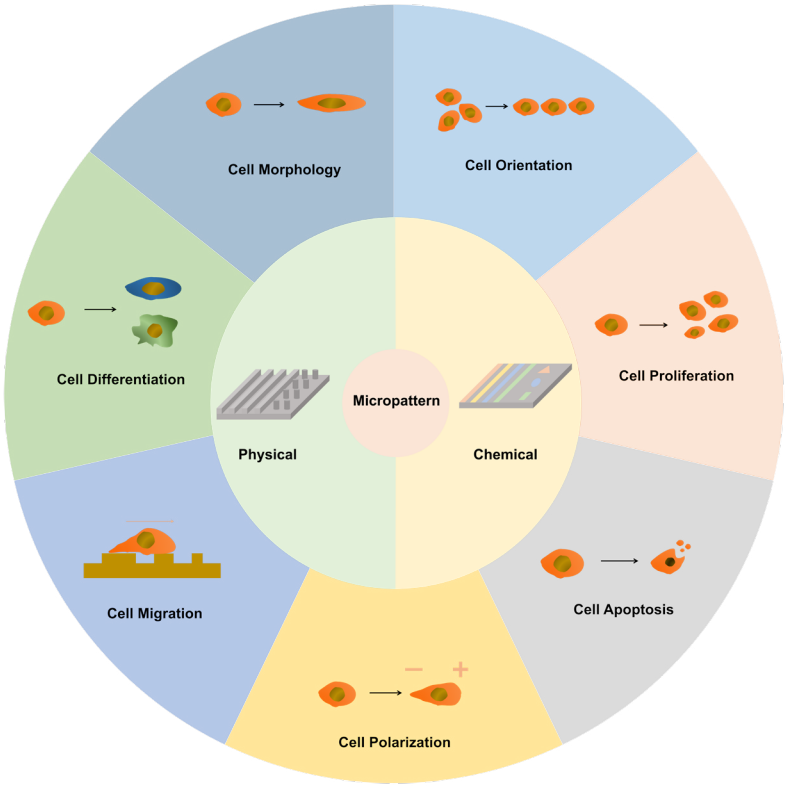

Figure 1. **Overview of Cellular Responses to Micropatterning**. Micropatterns are categorized into physical and chemical micropatterning techniques, both of which have the capacity to modulate various aspects of cellular behavior. These include alterations in cell morphology, orientation, proliferation, apoptosis, migration, polarity, and differentiation.

amalgamates surface chemistry and materials science, is employed to create micro/nanoscale morphologies on material surface or utilize specific chemicals to form specific patterns to control the shape, size, and arrangement of cell adhesion. This advanced technology facilitates research in tissue engineering, regenerative medicine, and biosensors [15]. Micropatterned material can mimic physical and chemical signals of in situ cells, providing inspiration for using micropatterning to modulate cell behavior. Harrison [16] first identified the influence of solid substrates on cell morphology and movement. In 1964, Curtis et al. [17] pioneered the active use of physical factors to modulate cellular behavior. In 1967, Cater et al. [18] applied techniques from electronics to confine single cells to diminutive adhesion islands, which were utilized to decipher cell behavior. In recent years, researchers have employed various methods such as soft lithography and microcontact printing to construct the desired micropatterns [19-22], achieving regulations of various cellular behaviors including cell orientation, migration, and polarity [21,23-26].

In this review, we categorize micropatterns based on the commonalities and disparities in their construction methods. We then focus on reviewing eight aspects of cell behavior regulated by micropatterns (Figure 1), with the aim of providing valuable insights for subsequent researchers in this field.

Classification of Micropattern

Different types of micropatterns elicit varying alterations in cellular functions, making the selection of an appropriate micropattern crucial when studying cell function. There are two primary types of micropatterning approaches to stimulate cell growth (Figure 2): physical micropatterning, which constructs topological microstructures to confine cell adhesion and growth to specific structures, and chemical micropatterning, where light-induced protein molecules are adsorbed to form specific patterns, thus inducing cell growth on these specific patterns.

Physical Micropatterning

Physical micropatterning primarily involves the formation of micro-pits and micro-grooves of varying shapes and sizes on the surface of matrix materials such as polydimethylsiloxane (PDMS) and hydrogels. This restricts cell growth spatially and guides cells to extend in

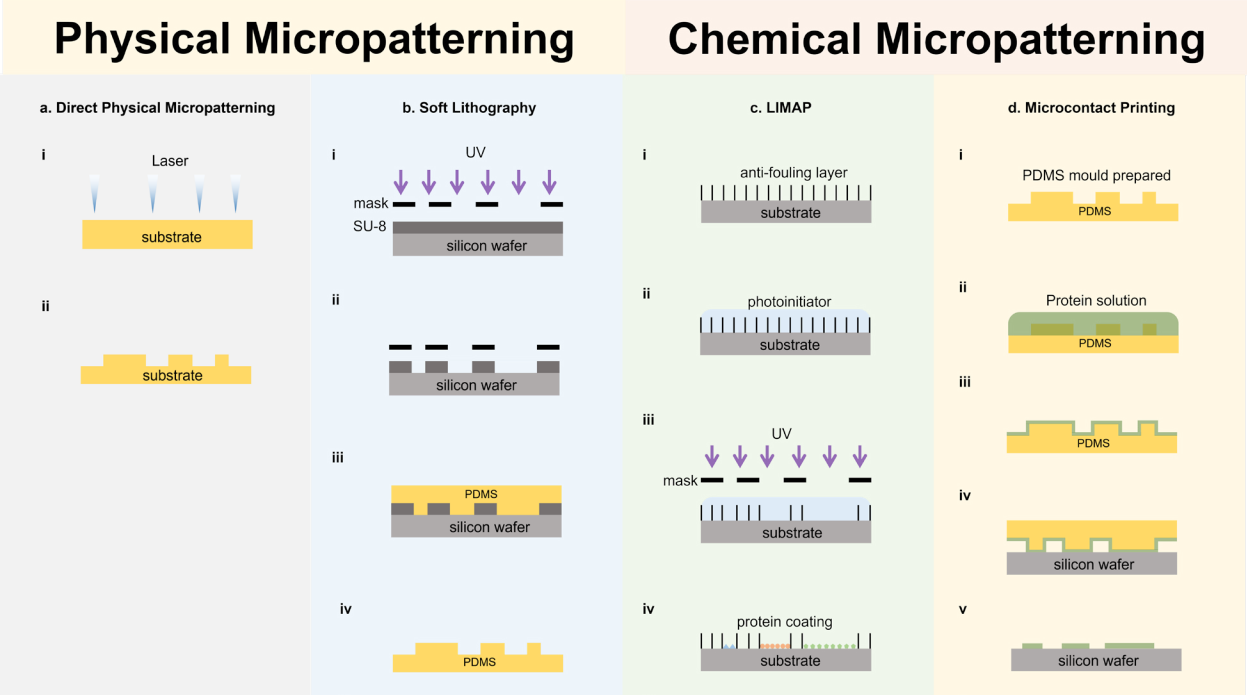

Figure 2. **Methods for Fabricating Micropatterns**. There are several methods employed for micropattern fabrication, including: (**a**) Direct Physical Micropatterning: This technique involves creating micropatterns directly on a substrate using methods such as lasers. (**b**) Soft Lithography: Soft lithography is a physical micropatterning method that begins with forming a specific shape of SU-8 photoresist as a master mold by exposing it to UV light through a mask. The micropatterned mold is then obtained by casting with PDMS and curing with a hot plate. (**c**) LIMAP (Light-Induced Molecular Adsorption Patterning): LIMAP is a chemical micropatterning technique used for protein adhesion. It involves degrading specific shapes of anti-fouling coatings through UV light exposure in the presence of photoinitiators. (**d**) Microcontact Printing: This chemical micropatterning method entails coating a layer of adherent proteins on a pre-prepared PDMS mold, which is then imprinted onto a substrate, resulting in protein micropatterning on the substrate.

the intended direction [27,28]. Physical micropatterns are currently constructed in two main ways: directly micropattern the material to form a specific morphology, such as using femtosecond laser etching to create nanotextured micropatterns on polyimide artificial lens surfaces [29], and indirect preparation of micropatterns using soft lithography. The latter method uses the SU-8 photoresist obtained by UV lithography as the master mold, with the micropatterned mold obtained after casting and hot plate curing using PDMS [30]. The master mold and the substrate material can be adapted to the experimental needs, such as using nickel molds to shape micro-patterns on the thermoplastic polyurethane surface [31]. Additionally, micro-slots and micro-pits can be docked and bonded to form three-dimensional physical microstructures, offering the possibility of three-dimensional cell research [32].

Chemical Micropatterning

Chemical micropatterning involves the precise manipulation of cell alignment and protein adsorption by constructing adhesive coatings of various shapes on substrate materials. There are two commonly used methods for fabricating chemical micropatterns.

The first method is referred to as light-induced molecular adsorption of proteins (LIMAP). It involves covering the substrate material surface with a layer of photoreactive material, such as polyvinyl alcohol (PVA), and adding a photoinitiator. A predesigned photomask is then applied, and specific areas of the coating are degraded using UV light irradiation. The adhesion protein selectively adheres to the areas degraded by UV light, resulting in the formation of an adhesion micropattern with a specific pattern [33-35].

The second method is microcontact printing. This method involves preparing a PDMS elastic stamp with a desired shape using soft lithography. The stamp is then coated with the desired protein composition and pressed onto a substrate to transfer the desired chemical pattern [36,37].

Researchers are currently exploring the combination of physical microstructures and chemical adhesion textures. For instance, they have been preparing polyethylene glycol (PEG) hydrogel microislands and modifying them with cell adhesion arginine-glycine-aspartate (RGD) li-

gands to create peptide micro/nanopatterns and generate composite micropatterns [38]. With advancements in chemistry and materials science, new methods are being developed, such as using ultrathin metal microstencils (UTmS), mild UV light and biocompatible bioconjugation chemistries, the patterning of low-molecular-weight ligands, and the utilization of hydrogels with photopatterned single-stranded DNA features for cell adhesion. These emerging techniques provide powerful tools for studying cell-material interactions at both the molecular and cellular levels [39-41].

MODULATING CELLULAR BEHAVIOR BY MICROPATTERNING

Micropatterning exerts a significant influence on a spectrum of cellular behaviors, including cell morphology and orientation, proliferation and apoptosis, migration, polarity, and differentiation. The impacts of physical micropatterning and chemical micropatterning on cell behaviors are summarized in Table 1 and Table 2, respectively.

Cell Morphology and Orientation

Cell morphology serves as a potent indicator of changes in cell function, phenotype, and signaling status [42]. The morphology and alignment of cells play critical roles in cytoskeletal reorganization, membrane protein translocation, nuclear gene expression, ECM remodeling, and tissue regeneration [43]. Studies have shown that cells can markedly elongate and align along the direction of micropatterns when cultivated in microgrooves/pits or on coated surfaces with analogous shapes. This alignment is observed not only in cell morphology but also in actin fibers and microtubules.

Physical micropatterning: Matthew W. Hagen et al. [44] prepared grooved polyurethane micropatterns ranging from 3-14 μm and seeded them with endothelial colony-forming cells (ECFCs). They observed significant alignment of cells with the angle of the micropattern at all spacings conditions, along with alignment of actin fibers and microtubules. In a study conducted by Park et al. [45], flexible poly(L-lactide-co-ε-caprolactone) (PLCL) was utilized to create 3D tubular structures for culturing neural cells. These structures were formed by rolling PLCL sheets with microgrooves of varying dimensions (ridge width × ridge height × groove width): 10 μm × 10 μm × 20 μm, 50 μm × 30 μm × 30 μm, and 100 μm × 50 μm × 30 μm. Neural cells exhibited significant elongation and alignment within these 3D micropatterns, as did the cytoskeleton. Recent studies have further revealed that only longer actin filaments are associated with changes in morphology [46].

To achieve dynamic changes in physical micropatterns, Puliafito et al. [47] designed an optically controlled micropillar array named Poly-DR1M, constructed from azopolymers, with a squared cross-section of 4 μm × 4 μm, a height of 1.3 μm, and pillar spacings of 5 μm, 7 μm, 9 μm, and 11 μm where each micropillar can be dynamically elongated based on the polarization direction of the laser, creating a real-time adjustable anisotropic surface. These changes in surface topography induced alignment responses in MDA-MB-231 cells, Madin-Darby canine kidney (MDCK), and actin filaments, guided by the cues provided by the micropatterns.

The aforementioned patterns are all in the micrometer scale. However, at the nanometer scale, micropatterns such as nanoscale-oriented liquid crystal lattices can also induce cell alignment [48].

Investigations into micropatterning have extended beyond cellular morphology to encompass the effects on nuclear morphology, attracting the attention of numerous researchers. For instance, in the case of bone marrow mesenchymal stem cells (BMSCs) cultivated on arrays of poly(lactic-co-glycolic acid) (PLGA) micropillars with spacing smaller than that of the cell nucleus (eg, 6 μm), the nucleus undergoes a notable and rapid phase of self-deformation followed by a slower phase of partial restitution of morphology. This restitution phase is contingent upon cytoskeletal function. This phenomenon has been examined across various cell types and has revealed nuclear size and cell-type dependencies. The distorted nuclei resulting from these micropatterns lead to chromosome repositioning and alterations in gene expression [49-52].

Chemical micropatterning: Sun et al. [53] developed gold stripe micropatterns (20 μm in width, inter-stripe distance from 5 to 80 μm) on a PEG hydrogel surface and seeded 3T3 cells. They observed that as the inter-stripe distance increased, the orientational order parameter, the ratio of long to short axes of a cell, and the occupation fraction of cells on stripes increased gradually, while the individual cell spreading area decreased. Salick et al. [54] employed microcontact printing to fabricate fibronectin and matrigel-coated square micropatterns with varying widths (15-115 μm) and aspect ratios (1:1-11:1). Their findings indicated that cardiomyocytes exhibited more pronounced aligned growth on micropatterns with narrow widths (ranging from 30 to 80 μm). The aspect ratio of cells was influenced by the diverse aspect ratios of the micropatterns, with cells elongating as the micropattern aspect ratio increased [55]. Employing the concept of dynamics, Vignaud et al. [56] used a tightly focused pulsed laser to degrade PEG coatings, enabling fibronectin adhesion and introducing new micropatterns composed of different arrangements of 300 nm diameter dots of adherent coatings alongside existing coatings, forming various shapes such as “I” and “V”. They ob-

Table 1. Summary of Cell Behaviors Controlled by Physical Micropatterns

Cell Behavior	Shape	Materials	Dimension	Cell	Details in Effect	Ref
Morphology and Orientation	Grooves	Polyurethane	3-14 μm peak-to-peak distance	ECFCs	Alignment of cells and cytoskeleton at all spacings.	[44]
	Grooves	PLCL	ridge width × ridge height × groove width: 10 μm × 10 μm × 20 μm, 50 μm × 30 μm × 30 μm, 100 μm × 50 μm × 30 μm	PC12 cells	Elongation and alignment of cells and cytoskeleton.	[45]
	Micropillar Array	Poly-DR1M	4 μm × 4 μm squared cross-section, 1.3 μm height, and pillar spacings of 5, 7, 9, and 11 μm	MDA-MB-231 and MDCK	Cells and actin filaments align in response to the micropatterns.	[47]
	Micropillar Arrays	PLGA	3 μm width, 6 μm spacing, heights from 0.2 μm to 5 μm, 6 μm or 7μm.	MSCs	Nuclear deformation observed in response to micropatterns.	[49-52]
Proliferation and Apoptosis	Equilateral triangular pores	Silicon	3–20 μm long sides	NIH-3T3	Cell proliferation rate decreases with decreasing micropore size.	[62]
	Hexagon	Nanofiber/ Hydrogel core–shell	500 μm, layer spacing 15-18 μm	HUVECs	Micropatterns promote cell proliferation and vascular network formation.	[63]
	Micropillar Arrays	PLGA	3 μm width, 6 μm spacing, 6 μm height	HeLa, HepG2, MC3T3-E1, and NIH3T3	Cell nuclei exhibit irregularities in shape and reduced size and proliferation.	[67]
Migration	Planar Zone; Micropillar Arrays; Micropits Arrays	PDMS	4 mm in diameter; 200 μm length, 200 μm width, and 500 μm height; curvatures from 0.02 to 0.002 μm-1 and depths of 10, 60, 100, and 200 μm	ECs, VSMCs	Interface characteristics influence cell traversal.	[76]
	Grooves	ORMOCOMP	3-75 μm widths, 0.5-5.0° divergence angles	NIH-3T3	Narrower grooves slow cell migration speed.	[77]
	Double-Pit of Square, Circles, Rectangles, Triangles, and Rhombuses	PLL-PEG	27.2-42.3 μm edge lengths	MDA-MB-231	Micropatterns affect cell occupancy rates.	[78]

	Microwells	PDMS	40, 25, 10 μm diameter	MSCs	Cell movement influenced by microwell size and tensile force.	[80]
	Grooves, Ridges, Pores	PDMS	the top layer features 2 μm grooves with 2 μm ridges, the middle layer comprises 14 μm deep pores, and the bottom layer consists of 30 μm wide and 15 μm deep grooves.	EBV-positive NPC43 cells	Microgroove morphology influences cell adhesion and traversal.	[81]
Differentiation	Micro- and Nano-Hybrid Surface	Hydroxyapatite	nano-rod with diameter of 70–100 nm, quadrate concave-convex surface with width and the space between the convex of 28 μm and 24 μm	MSCs	Structure promotes osteogenic differentiation.	[104]
	Micropillar Arrays	PLGA	3 μm width, 6 μm spacing, and ranging 0.8-6.4 μm heights	MSCs	Higher micropillars tend towards osteogenic differentiation.	[105]
	Concentric Circular Microgrooves	Polycaprolactone	200 μm diameter, and 20 μm width	RAW264.7	Concentric circular grooves inhibit osteoclast differentiation.	[106]
	Grooves	PDMS	10 μm width, and 3 or 10 μm depth	hPSCs	Microgroove morphology induces neuronal differentiation.	[107]
	Cylindrical and Circular Micropores	PEG	inner post diameter ranges from 50 to 250 μm, the outer diameter of 400 μm	BMEL 9A1 cells	Circular micropores promote biliary differentiation.	[109]
	Grooves	PDMS	100 and 200 μm widths	hESCs	Grooves promote myogenic differentiation.	[110]

served that hTERT-RPE1 cells changed their morphology in response to these micropatterns, with the actin fibers network underwent remodeling to support these cellular changes.

This behavior is not limited to two-dimensional (2D) culture. In one study, researchers created fibronectin stripe micropatterns (10 × 10 μm, width × spacing) on 2.5D convex and concave surfaces (curvatures between $\kappa = 1/2500$ and $\kappa = 1/125$ μm^{-1}) and found that both myofibroblasts and vascular endothelial cells (ECs) adhering to the protein stripes displayed alignment along the stripe [57]. Micropatterns in 3D have also been shown to influence cellular arrangement. Karzbrun et al. [58] found that laminin micropatterns with different widths significantly affected the morphology of the neural tube derived from human pluripotent stem cells (hPSCs). The width of the neural plate exhibited a linear relationship with the size of the micropattern. Micropatterns with a width of 150 μm resulted in a u-shaped neural fold with a single central hinge point, while wider micropatterns (>150 μm) carried two lateral hinges.

In both physical and chemical micropatterning, cells and their nucleus adapt their morphology to match the shape of the micropatterns, resulting in improved spreading and adhesion. The process can be dynamically regulated, allowing for dynamic changes in cell morphology. Specifically, narrower micropatterns have been shown to induce more pronounced cell elongation and alignment.

Table 2. Summary of Cell Behaviors Controlled by Chemical Micropatterns

Cell Behavior	Shape	Substrate	Coating	Dimension	Cell	Details in Effect	Ref
Morphology and Orientation	Stripe	PEG	Au	20 μm width, 5-80 μm inter-stripe distance	3T3 cells	Inter-stripe distance affects cell orientation and spreading area.	[53]
	Square and Stripe	Gold-coated glass	Poly (ethylene glycol) vs. Matrigel; Fibronectin	15-115 μm widths, and 1:1 -11:1 aspect ratio	hESC-CMs	Micropattern dimensions influence cell growth and aspect ratio.	[54]
	Dots with "I" and "V" Shapes	Polystyrene, Class	PEG vs. Fibrinogen	300 nm diameter	hTERT-RPE1 cells	Micropatterns induce changes in cell morphology and actin fibers.	[56]
	Stripe on 2.5D Convex and Concave Surface	PDMS	PLL + mPEG-SVA vs. Fibronectin	width × spacing, 10 × 10 μm; curvatures between $\kappa = 1/2500$ and $\kappa = 1/125\ \mu m^{-1}$	hmFBs, HUVECs	Cells align along protein stripes.	[57]
	Square	PDMS	PLL-g-PEG vs. Laminin	0-1500 μm width	hPSCs	Micropattern width affects neural plate development.	[58]
Proliferation and Apoptosis	Circular Microisland	Gold coated glass	M-PEG-Si (OMet)3 vs. RGD ligands	10-100 μm diameters	MSCs, EF, HeLa, HCvEpC, and NIH3T3 cells	Larger adhesion regions promote cell proliferation.	[68]
	Rectangular, Triangular, Square, and Round Shapes	Glass	Fibronectin	900 μm^2 area	MC3T3-E1 cells	Proliferation rate varies with micropattern shape.	[69]
	Stripe	Silicon Rubber	Pluronic vs. Fibronectin	15, 30, and 60 μm widths	HUVECs	Stripe width influences apoptosis rates and cell elongation.	[70]
	Circular Microisland	PEG	RGD	4μm-100 μm diameters	BMSCs, MC3T3-E1, NIH3T3	Smallest non-apoptotic cell area related to cell type and adhesion capacity.	[71]
	Circles and Circles with Rectangular Branches	Silicon	Nonadhesive comb polymer	1 and 0.1 circularities; 314, 628, 1256, or 2512 μm^2 size	MSCs	Micropattern area and roundness impact osteogenesis and apoptosis.	[72,73]

Migration	Droplet-Shaped Island	Gold-coated glass	HSC11-EG6 vs. Fibronectin	3 μm at the tip and 20 μm at the blunt end of the width of the teardrop	MCF-10A cells	Micropattern spacing influences migration direction.	[82]
	Straight, wavy and combinatory stripes	Gold-coated glass	PEG vs. RGD	4-μm widths straight microstripes, 20 μm width and arc radius of 20, 50 and 150 μm wavy microstripes, and combinatory microstripe pairs with 20 μm width and 50-400 μm arc radius.	SCs, NIH3T3, HeLa cells	Cells migrate along microstripes; linear stripes promote fastest migration.	[84]
Polarization	Circular Microisland	Glass	Matrigel	500 μm in diameter	hPSCs	Cells exhibit polarity differences at the edge and center.	[87]
	Teardrop-Shaped Microisland	Glass	PLL-g-PEG vs. Fibronectin	islands of 1 μm, 3 μm and 5 μm in diameter or fully FN-covered teardrop	MEFs	Microisland shape influences cell spreading and polarity.	[89]
	Circular Ring	Gold-coated glass	Ethylene glycol vs. Fibronectin	250 μm inner diameter and 200 μm distance between the inner and outer boundary	11 cell types	Chirality formation depends on cell phenotype and migration mechanism.	[90,91]
	Stripe	Hyaluronic Acid-Acrylamide Hydrogel	RGD	10-400 μm widths	bEnd.3 cells	Micropattern width influences chiral bias.	[93]
	Teardrop-Like Micropatterns	Gold-coated glass	RGD, RGE	short drop of 150 μm × 100 μm, long drop of 200 μm × 80 μm	MDCK cells	Cell polarity affected by micropattern shape and proteins.	[94]
Differentiation	Circular, T- And Y-Shaped Microisland	PEG Patterned, Gold-Coated Titanium	Triethylene glycol mono-11-mercaptoundecyl ether vs. Fibronectin	about 100 μm in diameter	MSCs	Micropatterns influence differentiation toward osteogenic lineage.	[111]
	Circular Microisland	TCPS	AzPhPVA	20, 40, 60 and 80 μm diameters	MSCs	Larger spreading areas enhance osteogenic differentiation.	[112]

Concentric, Linear, Honeycomb-Like, Square, and Gem-Like Stripes	Titanium	UV functionalized TiO2 nanorods	30 μm width	MSCs	Linear stripes activate YAP pathway and promote osteogenic differentiation.	[114]
Rectangular Microisland	PEG	Au	900 μm^2 area; aspect ratios of 1, 2, and 8	MSCs	Aspect ratio affects lipogenic and osteogenic differentiation.	[115]
Square, Triangle and Star-Shaped Microisland	Au coated PEG	RGD	900 μm^2, aspect ratio of 1	MSCs	Micropattern shapes influence differentiation.	[116]
Circular Microdomains	Au coated PEG	RGD	30 μm diameter	MSCs	More contacts between cells promote differentiation.	[118]
Stripe	Glass	RGD and Spidroin	500-1000 μm widths	hWJ-MSCs	Specific stripe patterns promote chondrogenic differentiation.	[120]
Stripe	Au coated SiO2	PEG vs. RGD and E-cadherin	5-150 μm widths	MSCs	Stripe properties influence osteogenic differentiation.	[121]
Square Rectangular and Hexagonal Patterns	PET	RGD, BMP-2, and OGP	Square (25, 50 and 100 μm length; 9, 15.5 and 17 μm gap), Rectangular (50 μm length, 25 μm width, 12.5 μm gap), and Hexagonal (88 μm length, 76.2 μm width, 19 μm gap)	MSCs	Peptide combinations enhance osteogenic differentiation.	[122]
Square	Au-coated PEG	Alkanethiols with −CH3, −OH, −COOH, or −NH2	30-60 μm side length	MSCs	Surface properties affect chondrogenic differentiation.	[123]

Cell Proliferation and Apoptosis

Aberrations in cell arrest and proliferation during the cell cycle are pivotal contributors to the pathogenesis of a plethora of diseases, including cancers and neurodegenerative diseases [59]. Apoptosis, an integral process in organ development and cell homeostasis, is often implicated in several diseases, such as developmental disorders and cancers, when its regulation is impaired [60]. Given the ability of micropatterns to affect fine morphology, it provokes the question of whether morphological alterations can impact cell proliferation and apoptosis.

Physical micropatterning: The rate of cell proliferation is not only related to the size of the micropattern but also intimately associated with its shape. For instance, human mesenchymal stem cells (MSCs) grown on patterned polystyrene substrates exhibit slower metabolism and a reduced rate of proliferation compared to their counterparts grown on unpatterned surfaces [61]. Also, mouse embryonic fibroblasts (NIH-3T3) grown in triangular micropores on silicon surfaces ranging from 3-20 μm displayed a decline in cell proliferation rate as the micropore size decreased, possibly due to decrease in mechanical stress and lower expression of F-actin [62].

Certain specific morphologies or shapes of micropatterns have also been associated with cell proliferation. For instance, the multilayered hexagonal nanofiber/hydrogel core–shell structure within micropatterned scaffolds (with a diameter of approximately 500 μm and layer spacing of 15-18 μm) that have been shown to effectively promote the proliferation of human umbilical vein endothelial cells (HUVECs) and the formation of vascular networks [63]. Bionics offers an effective strategy for constructing micropatterns that promote cell proliferation. Leaf vein-like structure [64], teak wood leaf-like structure [65], and the natural skin-like structure [66] have been shown to enhance the rate of cell proliferation and induce tissue regeneration and wound healing.

Furthermore, micropatterning has been shown to influence the shape and size of the cell nucleus, consequently impacting cell proliferation. Ruili et al. [67] conducted experiments involving four different cell types, including HeLa, HepG2, MC3T3-E1, and NIH3T3, cultured on PLGA micropillars with a width of 3 μm, spacing of 6 μm, and height of 6 μm. There findings revealed that the nuclei of HeLa and MC3T3-E1 cells experienced irregularities in shape and reduction in size. This was accompanied by a decrease in chromatin density and a subsequent reduction in proliferative capacity.

Chemical micropatterning: The size of the adhesion region provided by chemical micropatterns also plays a role in cell proliferation. Yao et al. [68] conducted experiments using various cell types including progenitor cells, stem cells, and cancer cells, and exposed them to gold rounded microislands modified with RGD of different sizes, ranging from 10 μm to 100 μm in diameter. They observed cell proliferation and found that the size of the adhesion region had a direct correlation with cell proliferation. Specifically, larger adhesion regions resulted in better cell proliferation.

Moreover, the shape of the micropattern markedly impacts the rate of cell proliferation. By utilizing microcontact printing techniques to restrict osteoblasts to microislands coated with fibronectin of specific shapes (eg, rectangular, triangular, square, and round) with an area of 900 μm^2, it was observed that the proliferation rate of osteoblasts increased sequentially [69]. Subsequent work revealed that changes in cell shape led to alterations in nuclear morphology, which in turn altered the gene expression of IP3R1 and SERCA2, resulting in different intracellular calcium transient patterns, which were instrumental in determining the proliferation rate of osteoblasts [69].

Similar to proliferation, both the size and shape of the micropatterns exert a substantial influence on apoptosis. Wu et al. [70] cultured HUVECs on fibronectin strips of different widths (15, 30, and 60 μm) and observed the highest rate of apoptosis on the 15 μm strip, with rates decreasing progressively with each increase in strip width. When fluid shear stress (FSS, 12 ± 4 dyn/cm^2) was applied parallel to fibronectin strips, HUVECs demonstrated enhanced cell elongation, stress fibers and phosphorylated adherents spot kinase (p-FAK), alongside decreased constraints on apoptosis induction. Their study implies that apoptosis can be regulated by alterations in ECM patterning, anisotropic cell morphology, and mechanical forces.

Yan et al. [71] examined the relationship between apoptosis and the area of RGD circular microislands (ranging from 4 μm to 100 μm in diameter) and defined the smallest area (A*) at which cells did not undergo apoptosis. They found that A* was cell type-dependent and associated with adhesion capacity. For instance, A* was greater for BMSCs than for MC3T3-E1 and less than for NIH3T3 cells.

Jiao et al. [72] used photolithography to create circular silicon wafer patterns surrounded by non-adhesive comb polymers with different roundness (circularities of 1 and 0.1) and size (314, 628, 1256, or 2512 μm^2), as well as circles with rectangular branches, to examine the effect of ECM morphology on the differentiation of MSCs. Their results showed that MSCs grown on micropatterns with larger areas and less roundness exhibited increased osteogenesis rates, whereas MSCs confined to smaller areas tended towards apoptosis. Cells displaying high apoptotic levels showed reduced osteogenesis, a process regulated by the yes-associated protein (YAP) pathway. Building upon this, Jiao et al. [73] further investigated the combined effect of FSS (0.5 or 0.8 Pa) and micropat-

terning on apoptosis. They discovered that a larger adhesion area and branch-like patterning reduced apoptosis and promoted osteogenesis in MSCs, independent of the intensity of FSS loading. Conversely, they found that FSS upregulated both osteogenesis and apoptosis, irrespective of area and roundness.

Based on the above studies, it is evident that smaller micropatterns are associated with lower cell proliferation rates, regardless of whether they are physical or chemical micropatterns. While the influence of shape on cell proliferation has been demonstrated, the optimal shape that promotes proliferation remains unclear. It is plausible to explore bionic approaches to micropattern design as a potential avenue for further investigation.

Regarding apoptosis, smaller patterns or narrower strip widths were found to remarkably increase apoptosis rates. Furthermore, the application of FSS to cells confined within micropatterns has been shown to further enhance apoptosis rates.

Cell Migration

Cell migration, a complex and comprehensive process, plays an indispensable role in embryonic development, wound healing, ossification, immunity, and most notably, in the invasion of cancer cells [74,75].

Physical micropatterning: Wang et al. [76] established a cell migration model using a micropatterned PDMS biochip. This biochip consisted of three regions: a planar cell seeding zone (4mm in diameter), a cell migration control zone consisting of an array of micro-pillars (200 μm in length, 200 μm in width, and 500 μm in height), and a cell migration zone with an array of micro-pits (width ranging from 50 to 500 μm, representing curvatures from 0.02 to 0.002 μm^{-1} and depths of 10, 60, 100, and 200 μm). By analyzing the proportion of ECs and vascular smooth muscle cells (VSMCs) occupying the micro-pits at different time points, they assessed the difficulty of cell migration in specific micro-pits. Their results showed that the interface with a greater the depth or width, or lower curvature, posed a more significant challenge for cell traversal. Furthermore, they discerned that the different responses of cells to different interfaces depended on cell geometry and the cytoskeleton.

Yoon et al. [77] explored the migration speed and direction of NIH-3T3 cells using micropatterns composed of ORMOCOMP polymer with varying widths (ranging from 3 to 75 μm) and divergence angles (ranging from 0.5 to 5.0°) and found that the narrower the width, the slower the migration speed, and cells exhibited a tendency to move towards larger divergence angles.

Fink et al. [78] took a double-pit poly-L-lysine-PEG (PLL-PEG) micropattern to study cell migration. Square micropatterns featured edge lengths of 27.2-42.3 μm, while other shapes, including circles, rectangles, triangles, and rhombuses, have equivalent areas to the squares. In this setup, MDA-MB-231 cells had freedom of movement within the two micro-pits, and cell migration was evaluated based on the occupancy rate. The results demonstrated that for identical or anisotropic connected micro-pits, the occupancy rate of cells was solely affected by the area of the micro-pit, with larger areas promoting higher occupancy rates. Conversely, in anisotropic micro-pits such as triangles and rhombuses, the possibility of occupancy varied based on the polarization of cells.

By developing a Chemo-mechanical model and simulations, Fang et al. [79] found that cell migration patterns, including flowing chain, suspended propagating bridge, and rotating vortex, were modulated by micropatterned substrates and were dependent on the strength of force-cell adhesion and force-contraction feedback.

Yingning et al. [80] designed a quasi-3D PDMS platform consisting of large (40 μm in diameter), medium (25 μm in diameter), and small (10 μm in diameter) microwells, each consisting of an array of micropillars arranged in a ring. This platform permitted cyclic stretching to study cell behavior. They discovered that hMSCs primarily moved perpendicular to the tensile force's direction under the cyclic tensile force influence. Compared with the state without tensile force, hMSCs cultured in medium and small microwells exhibited slower movement, while those cultured in large microwells and on flat surfaces moved faster.

In terms of cell migration on 3D patterns, Liu et al. [81] designed a 3D PDMS platform to mimic ECM containing blood vessels for studying tumor metastasis. The platform is composed of three layers: the top layer features 2 μm grooves with 2 μm ridges, the middle layer comprises 14 μm deep pores, and the bottom layer consists of 30 μm wide and 15 μm deep grooves. Their results showed that EBV-positive NPC43 cells located closer to the sidewalls of the microgrooves had a larger adhesion area and were more able to cross the pores. They also found that pore shape and size affected the likelihood of cells traversing the pore, with deeper grooves allowing more cells to pass and shallower grooves hindering it.

Chemical micropatterning: Compared to physical micropatterning, chemical micropatterning has been less frequently employed in the exploration of cell migration. One notable study by Kushiro et al. [82] utilized micropatterns (20 μm in width and 80 μm in length) composed of droplet-shaped fibronectin island coatings (3 μm at the tip and 20 μm at the blunt end of the width of the teardrop) to investigate cell migration behavior. The distances between the non-adhesive gaps ranged from 0 to 10 μm. They discovered that MCF-10A epithelial cells consistently moved in the direction that allowed for the formation of lateral lamellar pseudopods. Moreover, they found that closer distances between micropatterns

enhanced the propensity for migration. To optimize cell movement, a combination of droplet-shaped micropatterns, which could regulate direction more effectively, and strip-shaped micropatterns, which better controlled speed, was utilized [83].

Xiang et al. [84] prepared three types of RGD microstripes on the PEG surface, including straight microstripes with widths ranging from 4 to 100 μm, wavy microstripes with a width of 20 μm and arc radius of 20, 50, and 150 μm, and combinatory microstripe pairs with a width of 20 μm and an arc radius ranging from 50 to 400 μm. They discovered that cells migrated along the guidance of these microstripes, with the cells moving more quickly on linear microstripes featuring approximately 20 μm width and an arc radius of 150 μm. The also investigated potential left-right asymmetric deviation in cell migration, finding that for primary rat MSCs, the counterclockwise migration speed was higher than the clockwise migration speed. However, no left-right asymmetric bias was observed for NIH3T3 and HeLa cells.

Overall, while physical micropatterning is more commonly employed for studying cell migration due to the richer spatial cues it provides in the 2.5D or 3D context, planar chemical micropatterns have also been investigated. Micropatterns have been found to influence both the speed and direction of cell migration, which are crucial aspects of this cellular process. Specifically, greater depth, width, and reduced curvature have been observed to decrease the rate of cell migration. Additionally, larger dispersion angles and the use of adhesion proteins have been shown to enhance the propensity for cell migration. Special phenomena such as left-right asymmetric during cell migration have also been of interest for investigation.

Cell Polarization

Polarity is a fundamental aspect of an organism, influencing cell growth, the development of structures, and differential responses to external stimuli. In multicellular organisms, cell polarity also governs intercellular communication, pattern formation, and cellular properties. Any abnormalities in polarity are lined to various pathological processes [85,86]. Cell polarity can be divided into single-cell polarity and collective cell polarity. The former encompasses asymmetry in cell morphology, cytoskeleton, organelles, focal adhesion, and spreading direction, while the latter involves the directional arrangement and directional migration of multiple cells. Depending on the orientation, cell polarity can be categorized as left-right polarity, anterior-posterior polarity, and apical-basal polarity, all of which can be influenced by micropatterning.

For cell polarity studies, chemically coated micropatterns are primarily utilized, with the pattern shape varying according to the objectives of the study.

Kim et al. [87] employed circular Matrigel micropatterns (500 μm in diameter) to study the polarity of hPSCs and found a position-dependent polarity difference between cells at the edge and the center, manifested as variations in gene expression and biological function. By adjusting the size of circular micropattern, the ratio of marginal to central cells can be altered, which in turn influences the ratio of polarized spinal cord-like organs (pSCOs) on the dorsal/ventral side [88].

Lee et al. [89] used teardrop-shaped fibronectin microislands (with diameters of 1 μm, 3 μm and 5 μm, as well as fully FN-covered teardrop micropatterns) to study the polarity of mouse embryonic fibroblasts, finding that cells spread faster on larger microislands. Adjustments to the teardrop-shaped microislands, making them larger at either end, resulted in cells preferentially spreading to the larger area of the microislands, with more focal adhesions being formed. They further demonstrated that geometrical cues guided intracellular polarization, determining directional cell migration through localized activation of Cdc4, with lamin A/C playing a crucial mediating role.

Wan et al. [90,91] used circular ring fibronectin micropatterns (with an inner diameter of 250 μm and a 200 μm distance between the inner and outer boundaries) to study cellular chirality in 11 different cell types. They observed that cellular chirality was dependent on cell phenotype rather than adhesion pattern and that chirality formation was related to the mechanism of cell migration at the border and was dependent on the function of the actin skeleton. They also found that ECs exhibited a clockwise or rightward chirality on the micropatterns, and the cytoplasmic center was also polarized to the right of the nucleus-centrosome axis. Further studies revealed that this property is associated with the permeability of ECs and the activation of protein kinase C [92].

Chirality of brain microvascular ECs has also been studied using RGD-coated micropattern stripes, revealing a negative chiral bias on micropatterns with widths of 10 ~ 400 μm, with the most pronounced negative bias on 100 μm wide micropattern [93].

Costa et al. [94] used teardrop-like RGD or arginine-glycine-glutamate (RGE) micropatterns of different lengths (short drop measuring 150 μm × 100 μm, long drop measuring 200 μm × 80 μm) to study the polarity of canine kidney cells (MDCK). They found that a larger proportion of MDCK cells were highly polarized at the tip of the teardrop, and the number of polarized cells in the longer teardrop pattern was significantly higher than in the short teardrop. They also found that E-cadherin and microtubules played a key role in the formation of cell polarity.

In addition, the use of micropatterns for studying cell polarization and its related mechanisms have become an effective approach. Researchers have identified microtubule detyrosination [95] and the localization of

Nucleus-Golgi axis [96] as factors associated with cell polarization.

Among the various shapes of chemical micropatterns, solid circles, concentric rings, and teardrops are the most commonly used. Solid circles primarily exhibit polarity differences within the interior and at the edges, whereas concentric rings display polarity variations due to differences in position and width, resulting in varying chirality. Unlike the symmetrical patterns described above, teardrop chemical micropatterns have been employed by researchers specifically for their asymmetry. In this case, cells exhibit stronger polarization at the tip of the teardrop pattern and tend to move towards the blunt end. These polarity or chirality differences are primarily attributed to the asymmetric distribution of actin and focal adhesions.

It is worth noting that UV light is sometimes used in the fabrication of certain chemical micropatterns by LIMAP. However, it has been observed that UV light can alter the stiffness of the substrate [97,98], and substrate stiffness has been demonstrated to influence cell polarity [99,100]. This introduces an additional variable that may impact the accuracy of conclusions drawn from such studies.

Cell Differentiation

Stem cells form the foundation of regenerative medicine and tissue engineering, with the regulation of stem cell fate having significant implications for cancer treatment [101,102]. Micropatterns featuring varying shapes have been widely employed to investigate the differentiation of various stem cells, particularly MSCs.

Physical micropatterning: Numerous studies have highlighted the role of biophysical cues in guiding cell differentiation [103]. Zhao et al. [104] engineered a hybrid micro- and nano-scale hydroxyapatite surface structure on bioceramics, combining nano-rods with diameters of 70–100 nm and micro-patterned quadrate concave-convex surfaces with widths and spacings of 28 μm and 24 μm, respectively, to mimic the bone matrix. They discovered that this structure enhanced the osteogenic differentiation of MSCs compared to structures composed of either micron or nano elements alone. The differentiation was associated with integrins, the BMP2 pathway, and intercellular communication.

Xiangnan et al. [105] established arrays of PLGA micropillars with a width of 3 μm, a spacing of 6 μm, and heights ranging from 0.8 to 6.4 μm, and found that MSCs cultured on taller micropillars exhibited a more pronounced reduction in cytoskeletal tension, nuclear changes, and a tendency towards osteogenic differentiation.

Apart from MSCs, researchers have also fabricated polycaprolactone surfaces featuring concentric circular microgrooves (with an external diameter of 200 μm and a width of 20 μm) to simulate the concentric structure of bone blocks under 2D conditions [106]. They found that concentric circular grooves significantly inhibited the differentiation of osteoblastic progenitors (RAW264.7) to osteoclasts compared with parallel-aligned linear microgrooves.

Hsu et al. [107] seeded hPSCs on PDMS microgrooves (10 μm in width, with depths of either 3 or 10 μm) and found that microgroove morphology can downregulate the Notch signaling pathway and induce differentiation toward neuronal lineage. In a high-throughput study investigating the effects of more than 2,000 different shapes of polystyrene (PS) micropatterns on human epidermal stem cell differentiation, it was found that micropattern preventing cell spreading favored differentiation. Irregular topographies promoted differentiation in spreading cells, while high coverage favored differentiation in round cells. Actin polymerization and actomyosin contraction were identified as key factors influencing how various micropatterns either promoted or inhibited differentiation [108].

Berg et al. [109] established cylindrical and circular PEG micropore platforms (with inner post diameter ranging from 50 to 250 μm and an outer diameter of 400 μm), finding that circular micropores were more effective in promoting biliary differentiation of hepatic progenitor cells than cylindrical ones. Human embryonic-derived mesodermal progenitors exhibited strong myogenic differentiation in the striated PDMS microgrooves (with widths of 100 μm and 200 μm) [110].

Chemical micropatterning: Certain micropatterns, although prepared using techniques like LIMAP or microcontact printing, have been shown to regulate cell fate through mechanical cues. For instance, Piroli et al. [111] constructed circular, T- and Y-shaped fibronectin micropatterned coatings and found that cells on circular patterns exhibited mixed osteogenic and adipogenic differentiation. Both T- and Y-shapes increased the proportion of osteogenic differentiation, with the Y-shape having a more significant effect.

Yang et al. [112] prepared circular polystyrene micropatterns of different sizes (diameters of 20, 40, 60, and 80 μm) to provide MSCs with varying spreading areas, and found that cells with larger spreading areas had a higher degree of osteogenic differentiation and maintained a longer differentiation phenotype. Similar findings were reported by Rong et al. [113], who concluded that larger cell size correlated with a greater inclination toward osteogenic differentiation.

Luo et al. [114] produced UV functionalized TiO_2 nanorods micropattern in various configurations, including concentric, linear, honeycomb-like, square, and gem-like stripes (each with a width of 30 μm) and demonstrated

that linear stripes could effectively activate the YAP pathway and induce osteogenic differentiation of MSCs.

Xiang et al. [115] restricted MSCs to rectangular RGD micropatterns with different aspect ratios (each with the same area of 900 μm^2; aspect ratios of 1, 2, and 8) and found that the degree of lipogenic differentiation progressively decreased with increasing aspect ratio, with optimal osteogenic differentiation achieved at an aspect ratio of 2. Cellular tension associated with Rho-associated kinase (ROCK) pathway played a role in this phenomenon. Furthermore, Rong et al. [116] maintained cells at a fixed aspect ratio of 1 (with the same area of 900 μm^2) but varied their shapes through micropatterning, finding that rounded shapes were more likely to promote adipogenic differentiation, whereas star-shapes were more inclined to promote osteogenic differentiation, possibly due to the fact that rounded cells have a smaller perimeter compared to star-shaped ones.

Jo et al. [117] confined hPSCs to micropatterned islands of different sizes (ranging from 500 to 1000 μm in diameter) and confirmed that the colony size of hPSCs can affect the differentiation efficiency of human primordial germ cells-like cells. Investigating the differentiation of multicellular colonies, Jian et al. [118] connected circular RGD microislands, each with a diameter of 30 μm, to control the number of cells and the extent of cell contact. Their findings indicated that increased cell-cell contacts promoted differentiation, whether toward osteogenic or lipogenic lineages. Further research confirmed that hypoxic conditions promoted chondrogenic differentiation of MSCs on adherent microdomains more effectively than normoxic conditions, even when the degree of cell-cell contact remained constant [119].

In addition to purely mechanical signals such as shape and size, the chemical composition of micropatterned coatings can also influence cell differentiation. For instance, Barlian et al. [120] found that 1000 μm strips made with RGD-containing spidroin promoted chondrogenic differentiation of human Wharton's jelly MSCs (hWJ-MSCs) with increased expression of both SOX9 and type 2 collagen.

Saux et al. [121] prepared monofunctional striated surfaces with either RGD or E-cadherin and bifunctional surfaces with both RGD and E-cadherin spaced apart and with different stripes widths (ranging from 5 to 150 μm). When MSCs were seeded on these surfaces, they found that the E-cadherin monofunctional surface showed less osteogenic differentiation compared to the mono- and bi-functional surfaces with RGD, demonstrating the critical role of RGD in osteogenic differentiation. They also found that narrower stripes promoted osteogenic differentiation on the E-cadherin monofunctional surface. This promotion was not evident on the RGD monofunctional surface but was more significant on the bifunctional surface.

Padiolleau et al. [122] used a similar approach to study MSCs, besides they used a combination of RGD, BMP-2, and OGP to shape square (with a length of 25, 50 and 100 μm and a gap of 9, 15.5 and 17 μm), rectangular (with a length of 50, a width of 25 μm, and a gap of 12.5 μm) and hexagonal (with a length of 88 μm, a width of 76.2 μm, and a gap of 19 μm) patterns. They used RUNX2 and Colla1 as markers and found that all sizes, shapes, and protein combinations of the patterns promoted osteogenic differentiation.

Additionally, it has also been suggested that the effect of chemical composition on cell differentiation may be indirect. Bin et al. [123] seeded MSCs on surfaces coated with alkanethiols featuring one of four functional end groups (−CH3, −OH, −COOH, and −NH2). Neutral surfaces (-CH3 and -OH) adsorbed fewer proteins from the cell culture medium, leading to reduced cell spreading and a higher degree of chondrogenic differentiation than charged surfaces (-COOH and -NH2). However, when the cells were restricted to an extended region of the same size (squares of side lengths of 30 or 60 μm), the type of functional group had no significant effect on cell differentiation.

In summary, the studies suggest that micropatterns with smaller roundness, larger aspect ratio, longer perimeter, more branches, larger spreading area, stronger restrictions, and increased intercellular contacts tend to promote the osteogenic differentiation of MSCs. Micropatterns that mimic the growth microenvironment can induce the differentiation of stem cells towards specific cell types within that microenvironment. Furthermore, the inclusion of pro-adhesion molecules like RGD or E-cadherin within micropatterns has been shown to effectively enhance the osteogenic differentiation of MSCs.

It is worth noting that UV light exposure can alter the stiffness of the matrix, which has been demonstrated to influence cell differentiation [124,125]. Moreover, some studies have employed titanium dioxide (TiO_2) as a substrate. Nevertheless, it has been observed that the stiffness and other mechanical properties of cells may be altered when they grow on TiO_2 surfaces subsequent to UV irradiation [126,127]. The precise impact of these alterations on cell differentiation remains unclear and requires further investigation.

Other Cellular Biological Activities

Beyond the cellular behaviors discussed above, micropatterns have been found to influence a range of other cellular behaviors, including cell secretion [128,129], cell adhesion [130,131], intercellular communication [132], dedifferentiation [133], and gene transfection efficiency [134-136]. The underlying mechanisms of these behaviors and their relationship with micropatterns warrant

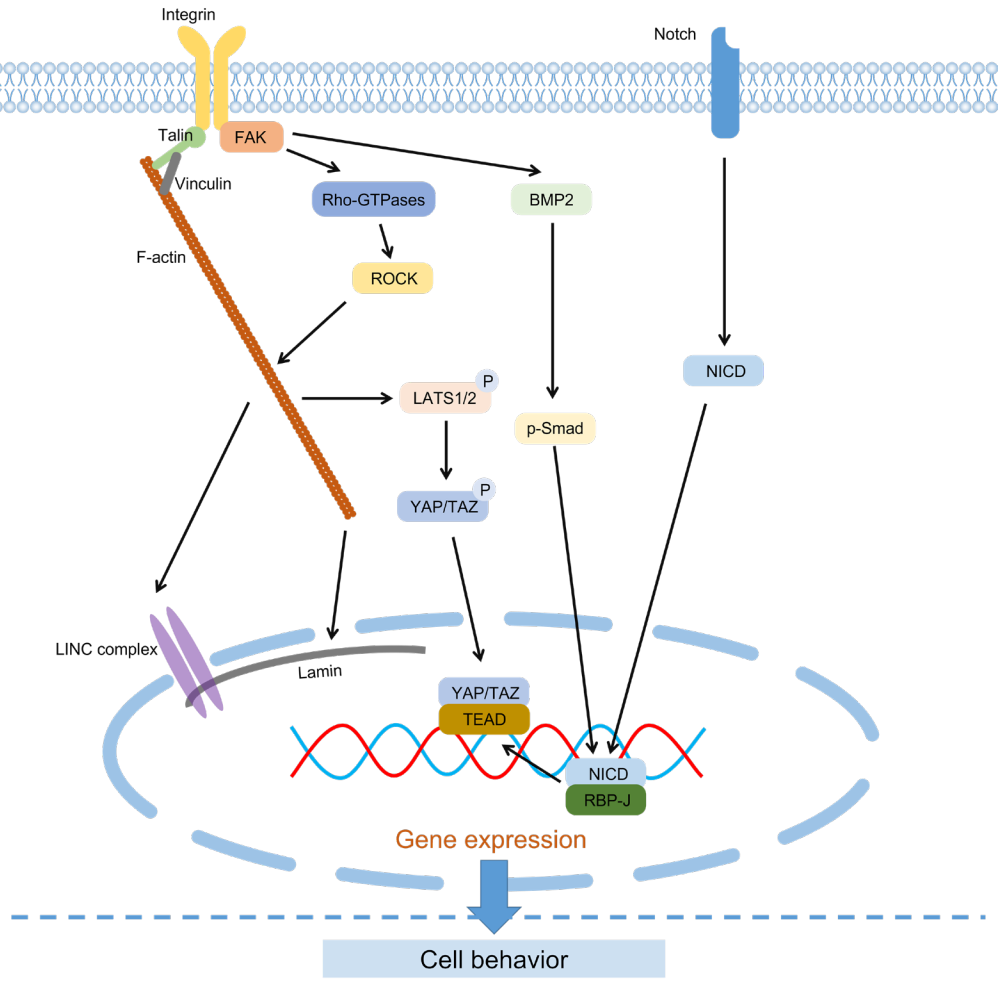

Figure 3. **Mechanisms Underlying Micropatterning-Mediated Regulation of Cell Behavior**. Micropatterning can influence cell behavior through various mechanisms, including: Integrin Signaling: Integrins sense mechanical signals from external micropatterns and recruit proteins like Talin and vinculin, thereby regulating F-actin assembly. This leads to cytoskeletal remodeling and consequent changes in cell behavior. Focal Adhesion Kinase (FAK) and Rho-associated kinase (ROCK) Pathway: Integrins transmit mechanical signals to FAK, which activates the ROCK signaling pathway. This pathway further regulates F-actin dynamics, impacting cell behavior. FAK can also activate the BMP2 signaling pathway, influencing gene expression through p-Smad phosphorylation. LATS1/2 Activation: F-actin's influence extends to the activation of LATS1/2, which governs the phosphorylation of YAP/TAZ. This phosphorylation determines whether YAP enters the nucleus and binds to TEAD, ultimately affecting gene expression. The LINC complex and Lamin also play pivotal roles in this process. Notch Signaling: Micropatterning can also modulate cell behavior through the Notch signaling pathway. Notch activation results in the production of Notch intracellular domain (NICD), which can bind to DNA binding protein RBP-J (also known as CSL or CBF1) to regulate gene expression. These intricate mechanisms collectively contribute to the regulation of various cellular behaviors in response to micropatterns, providing a deeper understanding of the cellular responses observed in micropatterning experiments.

further investigation.

Micropatterns can also impact the unique behaviors of certain cell types. For instance, in immune cells, micropatterns can regulate the phenotype of macrophages [137,138] and modulate T-cell activation [139]. In the case of neuronal cells, micropatterning can stimulate peripheral nerve morphogenesis [140] and enhance peripheral nerve regeneration [141-143]. Moreover, micropatterns can control the fusion of osteoclast precursors [144], and regulate the energy metabolism and cellular contractility of vascular smooth muscle cells [145].

In summary, the influence of micropatterns on cellular behaviors and function presents a broad and rich field for future research.

CONCLUSIONS AND OUTLOOK

Our manuscript offers a comprehensive summary

of the multifaceted effects of various micropattern types on cellular behaviors, encompassing a wide range of biological properties such as cell morphology, orientation, proliferation, apoptosis, migration, polarity, and differentiation. However, it is essential to acknowledge that micropatterns have the potential to influence cellular behaviors beyond these aspects. They can modulate physiological processes within individual cells and orchestrate intricate intercellular interactions through mechanical, chemical, and cell-to-cell stimuli. This aspect, ripe with potential, warrants further in-depth research.

Our review of the referenced studies reveals a prevalent use of simplistic micropatterns, such as stripes, circles, and squares, arranged in parallel, array, or radial configurations. The chemical modifications applied to these micropatterns primarily involve cell adhesion promoters such as fibronectin and RGD peptide. Recent research, however, has shown a growing interest in chirality, a factor known to influence cell behavior [146]. Innovative efforts are underway to integrate chirality into micropatterns [35], a trend we expect to intensify in the future. Another promising direction for micropattern design is biomimetic design [147], which can be tailored to the cellular environment for optimal regulatory effects or used as an in vitro model for exploring cell behavior regulatory mechanisms. Beyond adhesion-promoting substances [148], there is an untapped potential to incorporate a wider range of substances into micropatterns for cellular behavior regulation.

Micropatterning can be broadly classified into physical micropatterning and chemical micropatterning. With the progression of research, physical micropatterning has evolved from 2D to 2.5D and even 3D. However, chemical micropatterning has remained limited to the 2D level due to technical constraints. To achieve more intricate regulation of cellular behavior at the 3D level, there is a need to merge chemical micropatterning with physical micropatterning. This represents a promising direction for future researchers to explore.

The breadth of research reviewed herein underscores the remarkable potential of micropatterns in modulating cellular behaviors, demonstrating their significant applicative value. Notably, micropatterns hold great promise in the field of tissue engineering, where they could be utilized for controlled cell arrangement to facilitate tissue and organ formation. Moreover, micropatterns could be applied to implant surfaces to regulate cell secretion, promote the release of beneficial substances, and mitigate adverse postoperative reactions. In addition, micropatterns could induce selective cell adhesion and rapid directional movement, aiding in the design of materials that promote wound healing. Furthermore, micropatterns could stimulate cell differentiation, thereby enhancing the efficacy of stem cell therapy.

Indeed, micropatterns have proven to be powerful tools for influencing cellular behaviors, but there is a notable gap in understanding the underlying mechanisms of how these patterns exert their effects. While many studies have focused on the cellular responses to micropatterns, there is a need for deeper exploration into the mechanistic pathways involved (Figure 3).

Current research has primarily delved into the mechanotransduction of physical micropatterns and the YAP pathway as an example. Integrins, for instance, serve as sensors of mechanical signals from external physical micropatterns, triggering a cascade of events that involve proteins like Talin and vinculin, leading to F-actin assembly and cytoskeletal remodeling. This, in turn, affects cell behavior. Integrins also transmit mechanical signals to FAK, activating the ROCK signaling pathway, which further regulates F-actin dynamics. The activation of LATS1/2 by F-actin influences the phosphorylation of YAP and transcriptional coactivator with PDZ-binding motif (TAZ), determining whether YAP enters the nucleus to bind to transcriptional enhanced associate domain (TEAD) and ultimately affect gene expression. The Linker of Nucleoskeleton and Cytoskeleton (LINC) complex and Lamin also play crucial roles in this process [149-151].

In addition to the YAP signaling pathway, other studies have revealed that micropatterning can influence cell behavior through pathways such as BMP2 and Notch, with some interactions noted between Notch and YAP [152-154]. However, there remains a wealth of signaling pathways and mechanisms yet to be discovered by researchers in the context of micropatterning.

Addressing this research gap represents an exciting and promising direction for future investigations. Unraveling these mechanisms could further illuminate the pathways of cellular behavior regulation. Micropatterns, in this context, serve not only as tools for behavior regulation but also as invaluable probes for studying these mechanisms [90,92]. The challenge for future researchers is to harness these tools effectively for mechanistic studies.

Acknowledgments: This work is partly supported by the National Natural Science Foundation of China (12272246), the Key Research and Development Projects of Sichuan Province (2023YFS0075), and Radiation Oncology Key Laboratory of Sichuan Province Open Fund (2023ROKF02).

REFERENCES

1. Paul CD, Hung WC, Wirtz D, Konstantopoulos K. Engineered Models of Confined Cell Migration. Annu Rev Biomed Eng. 2016 Jul;18(1):159–80.
2. Friedl P, Alexander S. Cancer invasion and the micro-

environment: plasticity and reciprocity. Cell. 2011 Nov;147(5):992–1009.
3. Frantz C, Stewart KM, Weaver VM. The extracellular matrix at a glance. J Cell Sci. 2010 Dec;123(Pt 24):4195–200.
4. MacQueen L, Sun Y, Simmons CA. Mesenchymal stem cell mechanobiology and emerging experimental platforms. J R Soc Interface. 2013 May;10(84):20130179.
5. Eyckmans J, Boudou T, Yu X, Chen CS. A hitchhiker's guide to mechanobiology. Dev Cell. 2011 Jul;21(1):35–47.
6. Jaalouk DE, Lammerding J. Mechanotransduction gone awry. Nat Rev Mol Cell Biol. 2009 Jan;10(1):63–73.
7. Ye K, Wang X, Cao L, Li S, Li Z, Yu L, et al. Matrix Stiffness and Nanoscale Spatial Organization of Cell-Adhesive Ligands Direct Stem Cell Fate. Nano Lett. 2015 Jul;15(7):4720–9.
8. Peng Y, Liu QJ, He T, Ye K, Yao X, Ding J. Degradation rate affords a dynamic cue to regulate stem cells beyond varied matrix stiffness. Biomaterials. 2018 Sep;178:467–80.
9. Liu Q, Zheng S, Ye K, He J, Shen Y, Cui S, et al. Cell migration regulated by RGD nanospacing and enhanced under moderate cell adhesion on biomaterials. Biomaterials. 2020 Dec;263:120327.
10. Shen Y, Zhang W, Xie Y, Li A, Wang X, Chen X, et al. Surface modification to enhance cell migration on biomaterials and its combination with 3D structural design of occluders to improve interventional treatment of heart diseases. Biomaterials. 2021 Dec;279:121208.
11. Zhang H, Zhang W, Qiu H, Zhang G, Li X, Qi H, et al. A Biodegradable Metal-Polymer Composite Stent Safe and Effective on Physiological and Serum-Containing Biomimetic Conditions. Adv Healthc Mater. 2022 Nov;11(22):e2201740.
12. Yu Y, Wang X, Zhu Y, He Y, Xue H, Ding J. Is polydopamine beneficial for cells on the modified surface? Regen Biomater. 2022 Oct;9:rbac078. https://doi.org/10.1093/rb/rbac078.
13. Gao JM, Yu XY, Wang XL, He YN, Ding JD. Biomaterial-Related Cell Microenvironment in Tissue Engineering and Regenerative Medicine. Engineering (Beijing). 2022;13:31–45.
14. Cao D, Ding J. Recent advances in regenerative biomaterials. Regen Biomater. 2022 Dec;9:rbac098. https://doi.org/10.1093/rb/rbac098.
15. Yao X, Peng R, Ding J. Cell-material interactions revealed via material techniques of surface patterning. Adv Mater. 2013 Oct;25(37):5257–86.
16. Harrison RG. The cultivation of tissues in extraneous media as a method of morpho-genetic study. Anat Rec. 1912;6(4):167–94.
17. Curtis AS, Varde M. Control of Cell Behavior: topological Factors. J Natl Cancer Inst. 1964 Jul;33:15–26.
18. Carter SB. Haptotactic islands: a method of confining single cells to study individual cell reactions and clone formation. Exp Cell Res. 1967 Oct;48(1):189–93.
19. Falconnet D, Csucs G, Grandin HM, Textor M. Surface engineering approaches to micropattern surfaces for cell-based assays. Biomaterials. 2006 Jun;27(16):3044–63.
20. Zhou X, Boey F, Huo F, Huang L, Zhang H. Chemically functionalized surface patterning. Small. 2011 Aug;7(16):2273–89.
21. Ermis M, Antmen E, Hasirci V. Micro and Nanofabrication methods to control cell-substrate interactions and cell behavior: A review from the tissue engineering perspective. Bioact Mater. 2018 May;3(3):355–69.
22. Blin G. Quantitative developmental biology in vitro using micropatterning. Development. 2021 Aug;148(15):dev186387. https://doi.org/10.1242/dev.186387.
23. Wang WY, Pearson AT, Kutys ML, Choi CK, Wozniak MA, Baker BM, et al. Extracellular matrix alignment dictates the organization of focal adhesions and directs uniaxial cell migration. APL Bioeng. 2018 Dec;2(4):046107.
24. Pouthas F, Girard P, Lecaudey V, Ly TB, Gilmour D, Boulin C, et al. In migrating cells, the Golgi complex and the position of the centrosome depend on geometrical constraints of the substratum. J Cell Sci. 2008 Jul;121(Pt 14):2406–14.
25. Théry M, Racine V, Piel M, Pépin A, Dimitrov A, Chen Y, et al. Anisotropy of cell adhesive microenvironment governs cell internal organization and orientation of polarity. Proc Natl Acad Sci USA. 2006 Dec;103(52):19771–6.
26. Chen CS, Mrksich M, Huang S, Whitesides GM, Ingber DE. Geometric control of cell life and death. Science. 1997 May;276(5317):1425–8.
27. Zou J, Wu S, Chen J, Lei X, Li Q, Yu H, et al. Highly Efficient and Environmentally Friendly Fabrication of Robust, Programmable, and Biocompatible Anisotropic, All-Cellulose, Wrinkle-Patterned Hydrogels for Cell Alignment. Adv Mater. 2019 Nov;31(46):e1904762.
28. Shum AM, Che H, Wong AO, Zhang C, Wu H, Chan CW, et al. A Micropatterned Human Pluripotent Stem Cell-Based Ventricular Cardiac Anisotropic Sheet for Visualizing Drug-Induced Arrhythmogenicity. Adv Mater. 2017 Jan;29(1):1602448.
29. Seo Y, Kim S, Lee HS, Park J, Lee K, Jun I, et al. Femtosecond laser induced nano-textured micropatterning to regulate cell functions on implanted biomaterials. Acta Biomater. 2020 Oct;116:138–48.
30. Choi MJ, Park JY, Cha KJ, Rhie JW, Cho DW, Kim DS. Micropattern array with gradient size (μPAGS) plastic surfaces fabricated by PDMS (polydimethylsiloxane) mold-based hot embossing technique for investigation of cell-surface interaction. Biofabrication. 2012 Dec;4(4):045006.
31. May RM, Magin CM, Mann EE, Drinker MC, Fraser JC, Siedlecki CA, et al. An engineered micropattern to reduce bacterial colonization, platelet adhesion and fibrin sheath formation for improved biocompatibility of central venous catheters. Clin Transl Med. 2015 Feb;4(1):9.
32. Choi JS, Piao Y, Seo TS. Fabrication of a circular PDMS microchannel for constructing a three-dimensional endothelial cell layer. Bioprocess Biosyst Eng. 2013 Dec;36(12):1871–8.
33. Strale PO, Azioune A, Bugnicourt G, Lecomte Y, Chahid M, Studer V. Multiprotein Printing by Light-Induced Molecular Adsorption. Adv Mater. 2016 Mar;28(10):2024–9.
34. Melero C, Kolmogorova A, Atherton P, Derby B, Reid A, Jansen K, et al. Light-Induced Molecular Adsorption of Proteins Using the PRIMO System for Micro-Patterning to Study Cell Responses to Extracellular Matrix Proteins. J

Vis Exp. 2019 Oct;(152): https://doi.org/10.3791/60092-v.
35. Wang Y, Yang Y, Wang X, Yoshitomi T, Kawazoe N, Yang Y, et al. Micropattern-controlled chirality of focal adhesions regulates the cytoskeletal arrangement and gene transfection of mesenchymal stem cells. Biomaterials. 2021 Apr;271:120751.
36. Ryu JR, Jang MJ, Jo Y, Joo S, Lee DH, Lee BY, et al. Synaptic compartmentalization by micropatterned masking of a surface adhesive cue in cultured neurons. Biomaterials. 2016 Jun;92:46–56.
37. Thery M, Piel M. Adhesive micropatterns for cells: a microcontact printing protocol. Cold Spring Harb Protoc. 2009;2009(7):pdb prot5255. Epub 2010/02/12. https://doi.org/10.1101/pdb.prot5255..
38. Wang X, Li S, Yan C, Liu P, Ding J. Fabrication of RGD micro/nanopattern and corresponding study of stem cell differentiation. Nano Lett. 2015 Mar;15(3):1457–67.
39. Missirlis D, Baños M, Lussier F, Spatz JP. Facile and Versatile Method for Micropatterning Poly(acrylamide) Hydrogels Using Photocleavable Comonomers. ACS Appl Mater Interfaces. 2022 Jan;14(3):3643–52.
40. Song Y, Tian Q, Liu J, Guo W, Sun Y, Zhang S. A reusable single-cell patterning strategy based on an ultrathin metal microstencil. Lab Chip. 2021 Apr;21(8):1590–7.
41. Prahl LS, Porter CM, Liu J, Viola JM, Hughes AJ. Independent control over cell patterning and adhesion on hydrogel substrates for tissue interface mechanobiology. iScience. 2023 Apr;26(5):106657.
42. Prasad A, Alizadeh E. Cell Form and Function: Interpreting and Controlling the Shape of Adherent Cells. Trends Biotechnol. 2019 Apr;37(4):347–57.
43. Li Y, Huang G, Zhang X, Wang L, Du Y, Lu TJ, et al. Engineering cell alignment in vitro. Biotechnol Adv. 2014;32(2):347–65.
44. Hagen MW, Hinds MT. The Effects of Topographic Micropatterning on Endothelial Colony-Forming Cells. Tissue Eng Part A. 2021 Feb;27(3-4):270–81.
45. Park D, Kim D, Park SJ, Choi JH, Seo Y, Kim DH, et al. Micropattern-based nerve guidance conduit with hundreds of microchannels and stem cell recruitment for nerve regeneration. NPJ Regen Med. 2022 Oct;7(1):62.
46. Fink A, Doll CR, Yagüe Relimpio A, Dreher Y, Spatz JP, Göpfrich K, et al. Extracellular Cues Govern Shape and Cytoskeletal Organization in Giant Unilamellar Lipid Vesicles. ACS Synth Biol. 2023 Feb;12(2):369–74.
47. Puliafito A, Ricciardi S, Pirani F, Čermochová V, Boarino L, De Leo N, et al. Driving Cells with Light-Controlled Topographies. Adv Sci (Weinh). 2019 May;6(14):1801826.
48. Rojas-Rodríguez M, Fiaschi T, Mannelli M, Mortati L, Celegato F, Wiersma DS, et al. Cellular Contact Guidance on Liquid Crystalline Networks with Anisotropic Roughness. ACS Appl Mater Interfaces. 2023 Feb;15(11):14122–30.
49. Pan Z, Yan C, Peng R, Zhao Y, He Y, Ding J. Control of cell nucleus shapes via micropillar patterns. Biomaterials. 2012 Feb;33(6):1730–5.
50. Liu X, Liu R, Gu Y, Ding J. Nonmonotonic Self-Deformation of Cell Nuclei on Topological Surfaces with Micropillar Array. ACS Appl Mater Interfaces. 2017 Jun;9(22):18521–30.
51. Liu R, Liu Q, Pan Z, Liu X, Ding J. Cell Type and Nuclear Size Dependence of the Nuclear Deformation of Cells on a Micropillar Array. Langmuir. 2019 Jun;35(23):7469–77.
52. Liu R, Ding J. Chromosomal Repositioning and Gene Regulation of Cells on a Micropillar Array. ACS Appl Mater Interfaces. 2020 Aug;12(32):35799–812.
53. Sun J, Tang J, Ding J. Cell orientation on a stripe-micropatterned surface. Chin Sci Bull. 2009;54(18):3154–9.
54. Salick MR, Napiwocki BN, Sha J, Knight GT, Chindhy SA, Kamp TJ, et al. Micropattern width dependent sarcomere development in human ESC-derived cardiomyocytes. Biomaterials. 2014 May;35(15):4454–64.
55. Chen B, Co C, Ho CC. Cell shape dependent regulation of nuclear morphology. Biomaterials. 2015 Oct;67:129–36.
56. Vignaud T, Galland R, Tseng Q, Blanchoin L, Colombelli J, Théry M. Reprogramming cell shape with laser nano-patterning. J Cell Sci. 2012 May;125(Pt 9):2134–40.
57. van der Putten C, Buskermolen AB, Werner M, Brouwer HF, Bartels PA, Dankers PY, et al. Protein Micropatterning in 2.5D: An Approach to Investigate Cellular Responses in Multi-Cue Environments. ACS Appl Mater Interfaces. 2021 Jun;13(22):25589–98.
58. Karzbrun E, Khankhel AH, Megale HC, Glasauer SM, Wyle Y, Britton G, et al. Human neural tube morphogenesis in vitro by geometric constraints. Nature. 2021 Nov;599(7884):268–72.
59. Chiu J, Dawes IW. Redox control of cell proliferation. Trends Cell Biol. 2012 Nov;22(11):592–601.
60. Codispoti B, Makeeva I, Sied J, Benincasa C, Scacco S, Tatullo M. Should we reconsider the apoptosis as a strategic player in tissue regeneration? Int J Biol Sci. 2019 Jul;15(10):2029–36.
61. Beijer NR, Nauryzgaliyeva ZM, Arteaga EM, Pieuchot L, Anselme K, van de Peppel J, et al. Dynamic adaptation of mesenchymal stem cell physiology upon exposure to surface micropatterns. Sci Rep. 2019 Jun;9(1):9099.
62. Sunami H, Yokota I, Igarashi Y. Influence of the pattern size of micropatterned scaffolds on cell morphology, proliferation, migration and F-actin expression. Biomater Sci. 2014 Mar;2(3):399–409.
63. Li J, Zhang T, Pan M, Xue F, Lv F, Ke Q, et al. Nanofiber/hydrogel core-shell scaffolds with three-dimensional multilayer patterned structure for accelerating diabetic wound healing. J Nanobiotechnology. 2022 Jan;20(1):28.
64. Fang J, Liu H, Qiao W, Xu T, Yang Y, Xie H, et al. Biomimicking Leaf-Vein Engraved Soft and Elastic Membrane Promotes Vascular Reconstruction. Adv Healthc Mater. 2023 Jan;12(2):e2201220.
65. Satpathy A, Mohanty R, Rautray TR. Bio-mimicked guided tissue regeneration/guided bone regeneration membranes with hierarchical structured surfaces replicated from teak leaf exhibits enhanced bioactivity. J Biomed Mater Res B Appl Biomater. 2022 Jan;110(1):144–56.
66. He C, Yu B, Lv Y, Huang Y, Guo J, Li L, et al. Biomimetic Asymmetric Composite Dressing by Electrospinning with Aligned Nanofibrous and Micropatterned Structures for Severe Burn Wound Healing. ACS Appl Mater Interfaces. 2022 Jul;14(29):32799–812.
67. Liu R, Yao X, Liu X, Ding J. Proliferation of Cells with Severe Nuclear Deformation on a Micropillar Array. Lang-

muir. 2019 Jan;35(1):284–99.
68. Yao X, Liu R, Liang X, Ding J. Critical Areas of Proliferation of Single Cells on Micropatterned Surfaces and Corresponding Cell Type Dependence. ACS Appl Mater Interfaces. 2019 May;11(17):15366–80.
69. Tong J, Qi Y, Wang X, Yu L, Su C, Xie W, et al. Cell micropatterning reveals the modulatory effect of cell shape on proliferation through intracellular calcium transients. Biochim Biophys Acta Mol Cell Res. 2017 Dec;1864(12):2389–401.
70. Wu CC, Li YS, Haga JH, Kaunas R, Chiu JJ, Su FC, et al. Directional shear flow and Rho activation prevent the endothelial cell apoptosis induced by micropatterned anisotropic geometry. Proc Natl Acad Sci USA. 2007 Jan;104(4):1254–9.
71. Yan C, Sun J, Ding J. Critical areas of cell adhesion on micropatterned surfaces. Biomaterials. 2011 Jun;32(16):3931–8.
72. Jiao F, Zhao Y, Sun Q, Huo B. Spreading area and shape regulate the apoptosis and osteogenesis of mesenchymal stem cells on circular and branched micropatterned islands. J Biomed Mater Res A. 2020 Oct;108(10):2080–9.
73. Jiao F, Xu J, Zhao Y, Ye C, Sun Q, Liu C, et al. Synergistic effects of fluid shear stress and adhesion morphology on the apoptosis and osteogenesis of mesenchymal stem cells. J Biomed Mater Res A. 2022 Oct;110(10):1636–44.
74. Ridley AJ, Schwartz MA, Burridge K, Firtel RA, Ginsberg MH, Borisy G, et al. Cell migration: integrating signals from front to back. Science. 2003 Dec;302(5651):1704–9.
75. Franz CM, Jones GE, Ridley AJ. Cell migration in development and disease. Dev Cell. 2002 Feb;2(2):153–8.
76. Wang X, Wang H, He F, Zhang J. In Vitro Cell Migration through Three-Dimensional Interfaces of Varying Depths, Widths, and Curvatures on Micropatterned Polymer Surfaces. ACS Appl Bio Mater. 2020 Nov;3(11):7472–82.
77. Yoon SH, Kim YK, Han ED, Seo YH, Kim BH, Mofrad MR. Passive control of cell locomotion using micropatterns: the effect of micropattern geometry on the migratory behavior of adherent cells. Lab Chip. 2012 Jul;12(13):2391–402.
78. Fink A, Brückner DB, Schreiber C, Röttgermann PJ, Broedersz CP, Rädler JO. Area and Geometry Dependence of Cell Migration in Asymmetric Two-State Micropatterns. Biophys J. 2020 Feb;118(3):552–64.
79. Fang C, Yao J, Zhang Y, Lin Y. Active chemo-mechanical feedbacks dictate the collective migration of cells on patterned surfaces. Biophys J. 2022 Apr;121(7):1266–75.
80. He Y, Yu Y, Yang Y, Gu Y, Mao T, Shen Y, et al. Design and aligner-assisted fast fabrication of a microfluidic platform for quasi-3D cell studies on an elastic polymer. Bioact Mater. 2021 Dec;15:288–304.
81. Liu ZY, Zhang WG, Pang SW. Traversing behavior of tumor cells in three-dimensional platforms with different topography. PLoS One. 2020 Jun;15(6):e0234482.
82. Kushiro K, Chang S, Asthagiri AR. Reprogramming directional cell motility by tuning micropattern features and cellular signals. Adv Mater. 2010 Oct;22(40):4516–9.
83. Kushiro K, Asthagiri AR. Modular design of micropattern geometry achieves combinatorial enhancements in cell motility. Langmuir. 2012 Mar;28(9):4357–62.
84. Yao X, Ding J. Effects of Microstripe Geometry on Guided Cell Migration. ACS Appl Mater Interfaces. 2020 Jun;12(25):27971–83.
85. Bloch D, Yalovsky S. Cell polarity signaling. Curr Opin Plant Biol. 2013 Dec;16(6):734–42.
86. Butler MT, Wallingford JB. Planar cell polarity in development and disease. Nat Rev Mol Cell Biol. 2017 Jun;18(6):375–88.
87. Kim Y, Jang H, Seo K, Kim JH, Lee B, Cho HM, et al. Cell position within human pluripotent stem cell colonies determines apical specialization via an actin cytoskeleton-based mechanism. Stem Cell Reports. 2022 Jan;17(1):68–81.
88. Seo K, Cho S, Shin H, Shin A, Lee JH, Kim JH, et al. Symmetry Breaking of Human Pluripotent Stem Cells (hPSCs) in Micropattern Generates a Polarized Spinal Cord-Like Organoid (pSCO) with Dorsoventral Organization. Adv Sci (Weinh). 2023 Jul;10(20):e2301787.
89. Lee G, Han SB, Kim DH. Cell-ECM contact-guided intracellular polarization is mediated via lamin A/C dependent nucleus-cytoskeletal connection. Biomaterials. 2021 Jan;268:120548.
90. Wan LQ, Ronaldson K, Park M, Taylor G, Zhang Y, Gimble JM, et al. Micropatterned mammalian cells exhibit phenotype-specific left-right asymmetry. Proc Natl Acad Sci USA. 2011 Jul;108(30):12295–300.
91. Fan J, Zhang H, Rahman T, Stanton DN, Wan LQ. Cell organelle-based analysis of cell chirality. Commun Integr Biol. 2019 Apr;12(1):78–81.
92. Fan J, Ray P, Lu YW, Kaur G, Schwarz JJ, Wan LQ. Cell chirality regulates intercellular junctions and endothelial permeability. Sci Adv. 2018 Oct;4(10):eaat2111. https://doi.org/10.1126/sciadv.aat2111.
93. Porras Hernández AM, Tenje M, Antfolk M. Cell chirality exhibition of brain microvascular endothelial cells is dependent on micropattern width. RSC Adv. 2022 Oct;12(46):30135–44.
94. Costa P, Blowes LM, Laly AC, Connelly JT. Regulation of collective cell polarity and migration using dynamically adhesive micropatterned substrates. Acta Biomater. 2021 May;126:291–300.
95. Lavrsen K, Rajendraprasad G, Leda M, Eibes S, Vitiello E, Katopodis V, et al. Microtubule detyrosination drives symmetry breaking to polarize cells for directed cell migration. Proc Natl Acad Sci USA. 2023 May;120(22):e2300322120.
96. Vaidžiulytė K, Macé AS, Battistella A, Beng W, Schauer K, Coppey M. Persistent cell migration emerges from a coupling between protrusion dynamics and polarized trafficking. eLife. 2022 Mar;11:e69229.
97. Kim C, Young JL, Holle AW, Jeong K, Major LG, Jeong JH, et al. Stem Cell Mechanosensation on Gelatin Methacryloyl (GelMA) Stiffness Gradient Hydrogels. Ann Biomed Eng. 2020 Feb;48(2):893–902.
98. Liu YS, Chakravarthy RD, Saddik AA, Mohammed M, Lin HC. Supramolecular polymer/peptide hybrid hydrogels with tunable stiffness mediated by interchain acid-amide hydrogen bonds. RSC Adv. 2022 May;12(22):14315–20.
99. Gupta M, Doss BL, Kocgozlu L, Pan M, Mege RM, Callan-Jones A, et al. Cell shape and substrate stiffness drive actin-based cell polarity. Phys Rev E. 2019;99(1-1):012412. Epub 2019/02/20. https://doi.org/10.1103/Phys-

RevE.99.012412..
100. Das A, Adhikary S, Chowdhury AR, Barui A. Leveraging Substrate Stiffness to Promote Stem Cell Asymmetric Division via Mechanotransduction-Polarity Protein Axis and Its Bayesian Regression Analysis. Rejuvenation Res. 2022 Apr;25(2):59–69.
101. Tan F, Fang Y, Zhu L, Al-Rubeai M. Controlling stem cell fate using cold atmospheric plasma. Stem Cell Res Ther. 2020 Aug;11(1):368.
102. von Wangenheim KH, Peterson HP. The role of cell differentiation in controlling cell multiplication and cancer. J Cancer Res Clin Oncol. 2008 Jul;134(7):725–41.
103. Yim EK, Sheetz MP. Force-dependent cell signaling in stem cell differentiation. Stem Cell Res Ther. 2012 Oct;3(5):41.
104. Zhao C, Wang X, Gao L, Jing L, Zhou Q, Chang J. The role of the micro-pattern and nano-topography of hydroxyapatite bioceramics on stimulating osteogenic differentiation of mesenchymal stem cells. Acta Biomater. 2018 Jun;73:509–21.
105. Liu X, Liu R, Cao B, Ye K, Li S, Gu Y, et al. Subcellular cell geometry on micropillars regulates stem cell differentiation. Biomaterials. 2016 Dec;111:27–39.
106. Li M, Fu X, Gao H, Ji Y, Li J, Wang Y. Regulation of an osteon-like concentric microgrooved surface on osteogenesis and osteoclastogenesis. Biomaterials. 2019 Sep;216:119269.
107. Hsu CC, Serio A, Gopal S, Gelmi A, Chiappini C, Desai RA, et al. Biophysical Regulations of Epigenetic State and Notch Signaling in Neural Development Using Microgroove Substrates. ACS Appl Mater Interfaces. 2022 Jul;14(29):32773–87.
108. Zijl S, Vasilevich AS, Viswanathan P, Helling AL, Beijer NR, Walko G, et al. Micro-scaled topographies direct differentiation of human epidermal stem cells. Acta Biomater. 2019 Jan;84:133–45.
109. Berg IC, Mohagheghian E, Habing K, Wang N, Underhill GH. Microtissue Geometry and Cell-Generated Forces Drive Patterning of Liver Progenitor Cell Differentiation in 3D. Adv Healthc Mater. 2021 Jun;10(12):e2100223.
110. Hwang Y, Seo T, Hariri S, Choi C, Varghese S. Matrix Topographical Cue-Mediated Myogenic Differentiation of Human Embryonic Stem Cell Derivatives. Polymers (Basel). 2017 Nov;9(11):580.
111. Piroli ME, Jabbarzadeh E. Matrix Stiffness Modulates Mesenchymal Stem Cell Sensitivity to Geometric Asymmetry Signals. Ann Biomed Eng. 2018 Jun;46(6):888–98.
112. Yang Y, Wang X, Wang Y, Hu X, Kawazoe N, Yang Y, et al. Influence of Cell Spreading Area on the Osteogenic Commitment and Phenotype Maintenance of Mesenchymal Stem Cells. Sci Rep. 2019 May;9(1):6891.
113. Peng R, Yao X, Cao B, Tang J, Ding J. The effect of culture conditions on the adipogenic and osteogenic inductions of mesenchymal stem cells on micropatterned surfaces. Biomaterials. 2012 Sep;33(26):6008–19.
114. Lou Y, Sun M, Zhang J, Wang Y, Ma H, Sun Z, et al. Ultraviolet Light-Based Micropattern Printing on Titanium Surfaces to Promote Early Osseointegration. Adv Healthc Mater. 2023 Aug;12(21):e2203300.
115. Yao X, Peng R, Ding J. Effects of aspect ratios of stem cells on lineage commitments with and without induction media. Biomaterials. 2013 Jan;34(4):930–9.
116. Peng R, Yao X, Ding J. Effect of cell anisotropy on differentiation of stem cells on micropatterned surfaces through the controlled single cell adhesion. Biomaterials. 2011 Nov;32(32):8048–57.
117. Jo K, Teague S, Chen B, Khan HA, Freeburne E, Li H, et al. Efficient differentiation of human primordial germ cells through geometric control reveals a key role for Nodal signaling. eLife. 2022 Apr;11:e72811.
118. Tang J, Peng R, Ding J. The regulation of stem cell differentiation by cell-cell contact on micropatterned material surfaces. Biomaterials. 2010 Mar;31(9):2470–6.
119. Cao B, Li Z, Peng R, Ding J. Effects of cell-cell contact and oxygen tension on chondrogenic differentiation of stem cells. Biomaterials. 2015 Sep;64:21–32.
120. Barlian A, Saputri DH, Hernando A, Khoirinaya C, Prajatelistia E, Tanoto H. Spidroin striped micropattern promotes chondrogenic differentiation of human Wharton's jelly mesenchymal stem cells. Sci Rep. 2022 Mar;12(1):4837.
121. Le Saux G, Wu MC, Toledo E, Chen YQ, Fan YJ, Kuo JC, et al. Cell-Cell Adhesion-Driven Contact Guidance and Its Effect on Human Mesenchymal Stem Cell Differentiation. ACS Appl Mater Interfaces. 2020 May;12(20):22399–409.
122. Padiolleau L, Chanseau C, Durrieu S, Ayela C, Laroche G, Durrieu MC. Directing hMSCs fate through geometrical cues and mimetics peptides. J Biomed Mater Res A. 2020 Feb;108(2):201–11.
123. Cao B, Peng Y, Liu X, Ding J. Effects of Functional Groups of Materials on Nonspecific Adhesion and Chondrogenic Induction of Mesenchymal Stem Cells on Free and Micropatterned Surfaces. ACS Appl Mater Interfaces. 2017 Jul;9(28):23574–85.
124. He S, Lei P, Kang W, Cheung P, Xu T, Mana M, et al. Stiffness Restricts the Stemness of the Intestinal Stem Cells and Skews Their Differentiation Toward Goblet Cells. Gastroenterology. 2023 Jun;164(7):1137–1151.e15.
125. Sun Y, Liu J, Xu Z, Lin X, Zhang X, Li L, et al. Matrix stiffness regulates myocardial differentiation of human umbilical cord mesenchymal stem cells. Aging (Albany NY). 2020 Dec;13(2):2231–50.
126. Yamada M, Miyauchi T, Yamamoto A, Iwasa F, Takeuchi M, Anpo M, et al. Enhancement of adhesion strength and cellular stiffness of osteoblasts on mirror-polished titanium surface by UV-photofunctionalization. Acta Biomater. 2010 Dec;6(12):4578–88.
127. Vileno B, Lekka M, Sienkiewicz A, Jeney S, Stoessel G, Lekki J, et al. Stiffness alterations of single cells induced by UV in the presence of nanoTiO2. Environ Sci Technol. 2007 Jul;41(14):5149–53.
128. Li J, Zhang K, Yang P, Qin W, Li G, Zhao A, et al. Human vascular endothelial cell morphology and functional cytokine secretion influenced by different size of HA micro-pattern on titanium substrate. Colloids Surf B Biointerfaces. 2013 Oct;110:199–207.
129. Hisey CL, Hearn JI, Hansford DJ, Blenkiron C, Chamley LW. Micropatterned growth surface topography affects extracellular vesicle production. Colloids Surf B Biointer-

faces. 2021 Jul;203:111772.
130. Joshi A, Kaur T, Singh N. Exploiting Substrate Cues for Co-Culturing Cells in a Micropattern. Langmuir. 2021 Apr;37(16):4933–42.
131. Zheng S, Liu Q, He J, Wang X, Ye K, Wang X, et al. Critical adhesion areas of cells on micro-nanopatterns. Nano Res. 2021:1–13.
132. Xing F, Zhang P, Jiang P, Chen Z, Yang J, Hu F, et al. Spatiotemporal Characteristics of Intercellular Calcium Wave Communication in Micropatterned Assemblies of Single Cells. ACS Appl Mater Interfaces. 2018 Jan;10(3):2937–45.
133. Cao B, Peng R, Li Z, Ding J. Effects of spreading areas and aspect ratios of single cells on dedifferentiation of chondrocytes. Biomaterials. 2014 Aug;35(25):6871–81.
134. Wang Y, Yang Y, Wang X, Kawazoe N, Yang Y, Chen G. The varied influences of cell adhesion and spreading on gene transfection of mesenchymal stem cells on a micropatterned substrate. Acta Biomater. 2021 Apr;125:100–11.
135. Wang Y, Yang Y, Yoshitomi T, Kawazoe N, Yang Y, Chen G. Regulation of gene transfection by cell size, shape and elongation on micropatterned surfaces. J Mater Chem B. 2021 Jun;9(21):4329–39.
136. Wang Y, Wang N, Yang Y, Chen Y, Zhang Z. Cellular nanomechanics derived from pattern-dependent focal adhesion and cytoskeleton to balance gene transfection of malignant osteosarcoma. J Nanobiotechnology. 2022 Nov;20(1):499.
137. McWhorter FY, Wang T, Nguyen P, Chung T, Liu WF. Modulation of macrophage phenotype by cell shape. Proc Natl Acad Sci USA. 2013 Oct;110(43):17253–8.
138. Zhang B, Han F, Wang Y, Sun Y, Zhang M, Yu X, et al. Cells-Micropatterning Biomaterials for Immune Activation and Bone Regeneration. Adv Sci (Weinh). 2022 Jun;9(18):e2200670.
139. Sadoun A, Biarnes-Pelicot M, Ghesquiere-Dierickx L, Wu A, Théodoly O, Limozin L, et al. Controlling T cells spreading, mechanics and activation by micropatterning. Sci Rep. 2021 Mar;11(1):6783.
140. Cerri F, Salvatore L, Memon D, Boneschi FM, Madaghiele M, Brambilla P, et al. Peripheral nerve morphogenesis induced by scaffold micropatterning. Biomaterials. 2014 Apr;35(13):4035–45.
141. Uz M, Sharma AD, Adhikari P, Sakaguchi DS, Mallapragada SK. Development of multifunctional films for peripheral nerve regeneration. Acta Biomater. 2017 Jul;56:141–52.
142. Huang WC, Lin CC, Chiu TW, Chen SY. 3D Gradient and Linearly Aligned Magnetic Microcapsules in Nerve Guidance Conduits with Remotely Spatiotemporally Controlled Release to Enhance Peripheral Nerve Repair. ACS Appl Mater Interfaces. 2022 Oct;14(41):46188–200.
143. Zhang D, Li Z, Shi H, Yao Y, Du W, Lu P, et al. Micropatterns and peptide gradient on the inner surface of a guidance conduit synergistically promotes nerve regeneration in vivo. Bioact Mater. 2021 Jul;9:134–46.
144. Sun Q, Liu C, Bai X, Huo B. Cell-substrate traction force regulates the fusion of osteoclast precursors through cell-cell interaction. Biomech Model Mechanobiol. 2020 Apr;19(2):481–92.
145. Liu H, Liu Y, Wang H, Zhao Q, Zhang T, Xie SA, et al. Geometric Constraints Regulate Energy Metabolism and Cellular Contractility in Vascular Smooth Muscle Cells by Coordinating Mitochondrial DNA Methylation. Adv Sci (Weinh). 2022 Nov;9(32):e2203995.
146. Bao Y, Wu S, Chu LT, Kwong HK, Hartanto H, Huang Y, et al. Early Committed Clockwise Cell Chirality Upregulates Adipogenic Differentiation of Mesenchymal Stem Cells. Adv Biosyst. 2020 Oct;4(10):e2000161.
147. De Gregorio V, Imparato G, Urciuolo F, Netti PA. Micro-patterned endogenous stroma equivalent induces polarized crypt-villus architecture of human small intestinal epithelium. Acta Biomater. 2018 Nov;81:43–59.
148. Jeon O, Lee K, Alsberg E. Spatial Micropatterning of Growth Factors in 3D Hydrogels for Location-Specific Regulation of Cellular Behaviors. Small. 2018 Jun;14(25):e1800579.
149. Saraswathibhatla A, Indana D, Chaudhuri O. Cell-extracellular matrix mechanotransduction in 3D. Nat Rev Mol Cell Biol. 2023 Jul;24(7):495–516.
150. Kechagia JZ, Ivaska J, Roca-Cusachs P. Integrins as biomechanical sensors of the microenvironment. Nat Rev Mol Cell Biol. 2019 Aug;20(8):457–73.
151. Fu M, Hu Y, Lan T, Guan KL, Luo T, Luo M. The Hippo signalling pathway and its implications in human health and diseases. Signal Transduct Target Ther. 2022 Nov;7(1):376.
152. Shi H, Zhou K, Wang M, Wang N, Song Y, Xiong W, et al. Integrating physicomechanical and biological strategies for BTE: biomaterials-induced osteogenic differentiation of MSCs. Theranostics. 2023 May;13(10):3245–75.
153. Yang Y, Ni M, Zong R, Yu M, Sun Y, Li J, et al. Targeting Notch1-YAP Circuit Reprograms Macrophage Polarization and Alleviates Acute Liver Injury in Mice. Cell Mol Gastroenterol Hepatol. 2023;15(5):1085–104.
154. Zhou B, Lin W, Long Y, Yang Y, Zhang H, Wu K, et al. Notch signaling pathway: architecture, disease, and therapeutics. Signal Transduct Target Ther. 2022 Mar;7(1):95.